

## Photon-Noise Limited Performance in Aluminum LEKIDs

P. D. Mauskopf · S. Doyle · P. Barry · S. Rowe ·  
A. Bidead · P. A. R. Ade · C. Tucker · E. Castillo ·  
A. Monfardini · J. Goupy · M. Calvo

Received: 4 September 2013 / Accepted: 23 December 2013 / Published online: 14 January 2014  
© Springer Science+Business Media New York 2014

**Abstract** We have measured noise in aluminum lumped element kinetic inductance detectors (LEKIDs) in dark conditions at different base temperatures and with optical illumination from a variable temperature blackbody source. LEKIDs are photon-sensitive superconducting resonators coupled to planar transmission lines. We convert variations in the raw in-phase ( $e_I$ ) and quadrature ( $e_Q$ ) signals from a fixed frequency source transmitted through a transmission line coupled to the LEKID into a measure of the fluctuation in the resonant frequency of the LEKID ( $e_f$ ) using the measured electrical response of the resonator to a swept frequency source. We find that the noise of the LEKID in the dark has a constant frequency fluctuation level,  $e_f^0$  which is rolled off at a base temperature-dependent frequency corresponding to the quasiparticle lifetime in the device. Above this frequency, the noise is dominated by amplifier noise at a level a factor of 2–10 times lower than the low frequency white noise level depending on the quality factor of the resonator. The amplitude of this noise and the frequency cutoff agree well with the expected frequency fluctuation level from generation and recombination of thermal quasiparticles from a simple Mattis–Bardeen model. When we illuminate the device with a variable temperature blackbody source through a bandpass filter

---

P. D. Mauskopf (✉)  
School of Earth and Space Exploration and Department of Physics,  
Arizona State University, Tempe, AZ 85287, USA  
e-mail: mauskopf@asu.edu

P. D. Mauskopf · S. Doyle · P. Barry · S. Rowe · A. Bidead · P. A. R. Ade · C. Tucker  
School of Physics and Astronomy, Cardiff University, Cardiff, Wales CF24 3YB, UK

E. Castillo  
Instituto Nacional de Optica, Astrofisica y Electronica, Tonanzintla, Puebla, Mexico

A. Monfardini · J. Goupy · M. Calvo  
Institut Neel, Grenoble, France

centered at a frequency of 150 GHz, we observe a reduction in the quasiparticle lifetime and an increase in the level of frequency fluctuation noise as the blackbody temperature is increased. This indicates that the quasiparticle number is dominated by optically generated quasiparticles and that the noise in the device is dominated by photon noise.

**Keywords** Kinetic inductance · Generation–recombination noise · Photon noise · Quasiparticle lifetime

## 1 Introduction

Kinetic inductance detectors (KIDs) are superconducting electromagnetic resonators that change their resonant frequency and quality factor,  $q$ , in response to incident radiation. KIDs can be configured as distributed resonators where the resonant frequency is determined by the electrical length of a section of superconducting transmission line [1,2] or as lumped element resonators where the resonant frequency is determined by the product of a lumped inductance and capacitance [3]. Radiation is typically coupled to a distributed resonator using a planar antenna. Lumped element resonators are designed so that the inductor acts as a metal mesh absorber with an effective sheet impedance approximately equal to the normal resistance of the metal divided by the filling factor of the mesh. In both cases, the incident radiation breaks Cooper pairs and changes the relative populations of superconducting and non-superconducting charge carriers. This causes a change in the surface impedance of the superconducting material which contributes to the inductance and resistance of the resonator. Each KID is weakly coupled to a planar transmission line for readout. The resonant frequency,  $f_0$ , and quality factor,  $q$ , of a resonator can be measured by sweeping a tone in frequency through the resonant frequency of the KID and measuring the transmitted signal. In operation, the resonant frequency can be monitored by measuring the changes in the in-phase ( $I$ ) and quadrature ( $Q$ ) components of the transmitted signal as a function of time for a fixed input tone at the resonant frequency.

Astronomical imaging instruments using KIDs have been demonstrated or are in development for a variety of telescopes at mm-wave [4–6] and submm [7,8] wavelengths. These instruments ideally require photon noise limited detector performance under a range of optical loading conditions corresponding to different amounts of atmospheric and telescope emission at signal frequencies of  $\simeq 1$ –10 Hz typical of sky scanning speeds. Photon noise limited performance of antenna coupled distributed KIDs designed for 325 GHz has been demonstrated in the laboratory at signal frequencies of  $\geq 100$  Hz [9]. In this paper, we describe the laboratory characterization of devices in a lumped element KID array optimized for observations at 150 GHz in the New IRAM KIDs Array (NIKA) instrument. In particular, we measure the detector responsivity, response time and frequency noise level in dark conditions as a function of base temperature and with the detector illuminated with a variable temperature blackbody source as a function of optical loading at a fixed base temperature.

## 2 Experimental Details

The detector array consists of a  $12 \times 12$  array of pixels fabricated from a 15 nm aluminum film deposited on a  $350 \mu\text{m}$  thick high resistivity silicon wafer at PTA-Grenoble. Each pixel consists of an inductor patterned in the shape of a second order Hilbert curve designed to absorb 150 GHz radiation in both polarizations and an interdigital capacitor [10] coupled to an on-chip co-planar waveguide transmission line. The normal resistance of the aluminum film is measured to be  $4 \Omega$  per square and the kinetic inductance fraction is estimated to be 50 %. The chip was mounted in an aluminum holder and the readout transmission line was connected via wire bonds to intermediate grounded co-planar waveguide sections which were soldered to SMA connectors for input and output signals. The holder was mounted to a cold plate attached to a  $^3\text{He}$  sorption refrigerator with a base temperature of 245 mK and oriented with the bare silicon facing away from the cold plate and the side of the wafer with the detectors facing a solid aluminum backshort spaced  $500 \mu\text{m}$  from the detectors. The front side of the holder had a large hole for optical signals to enter into the detector array. For dark testing, this hole was blocked off with a blackened plate (Fig. 1).

For optical testing, the holder aperture was opened to the inside of the 245 mK volume and a 150 GHz metal mesh band pass filter was mounted in a 6 cm diameter aperture on the 245 mK radiation shield at a distance of 17 cm from the optical aperture in the chip holder. The inside of the 245 mK shield was painted with black paint and a black cylindrical baffle tube extended 8 cm downwards from the optical aperture to reduce the effects of scattered light through the filters. A second set of filters was mounted in a 7 cm aperture in a 4 K radiation shield outside of the 245 mK shield and a variable temperature 12 cm diameter blackbody source was mounted on the 60 K shield in front of the 4 K aperture. The signal from a detector was measured with a single pixel homodyne readout electronics providing 500 kHz sampling.

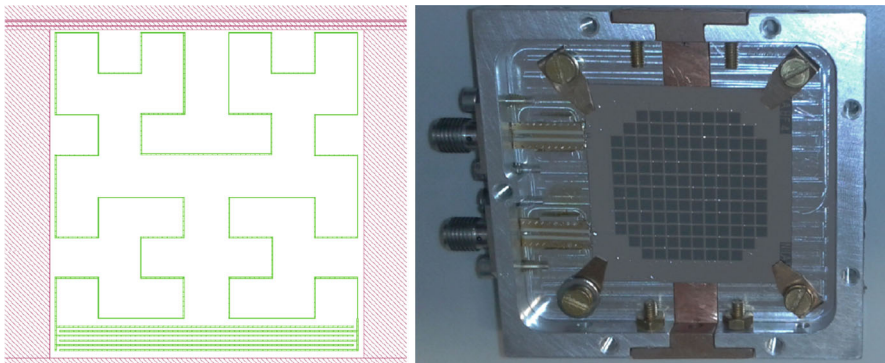


**Fig. 1** *Left* Geometry of a pixel in the NIKA 150 GHz array. The outer dimensions of the inductor are  $1,850 \mu\text{m} \times 1,850 \mu\text{m}$ . *Green* is the pixel and *red* is the transmission line and ground plane. The linewidth in the capacitor is  $8 \mu\text{m}$  with finger spacing of  $16 \mu\text{m}$ . The linewidth in the meander is  $4 \mu\text{m}$ . *Right* photograph of a mounted NIKA array. The entire structure is patterned from a 15 nm thick aluminum film deposited on a high resistivity silicon substrate. (Color figure online)

### 3 Results

We measured the complex transmission ( $S_{21} = I + iQ$ ) of the KID through the electronics as a function of frequency sweeping the source in frequency and measuring the amplitude of the in-phase ( $I$ ) and quadrature ( $Q$ ) signals. Examples of these sweeps for different base temperatures and optical loading conditions are shown in Fig. 2. The transmitted signal through a resonator can be approximated as,

$$S_{21} = 1 - \frac{q_r}{q_c} \frac{1}{1 + 2iq_r(f - f_0)/f_0} \quad (1)$$

where  $I = \text{Re}\{S_{21}\}$ ,  $Q = \text{Im}\{S_{21}\}$ ,  $q_c$  is the coupling quality factor for the resonator,  $q_r$  is the effective quality factor of the resonator and  $f_0$  is the resonant frequency. For the NIKA resonators,  $q_c = 32,000$  and  $q_r$  varies from 29,000 to 14,000 for base temperatures of 250–350 mK.

After each frequency sweep, we fixed the source frequency at a value close to the minimum of the magnitude of the  $S_{21}$  curve and obtained time stream data to measure the noise power spectral density. We maintained the readout source at the same power level during the noise measurements as in the sweeps. Dark noise spectra for the component of noise corresponding to fluctuations in the resonant frequency of the KID are shown in Fig. 3. The noise in a KID has contributions from random fluctuations in the generation and recombination of thermal quasiparticles (G–R noise), random fluctuations in the dielectric constant of the substrate due to fluctuating two-level systems (TLS noise) and amplifier noise. We calculate the noise power spectral density in terms of the fluctuations in resonant frequency using

$$e_f(\omega) = \frac{I(\omega) dI/df + Q(\omega) dQ/df}{(dI/df)^2 + (dQ/df)^2} \quad (2)$$

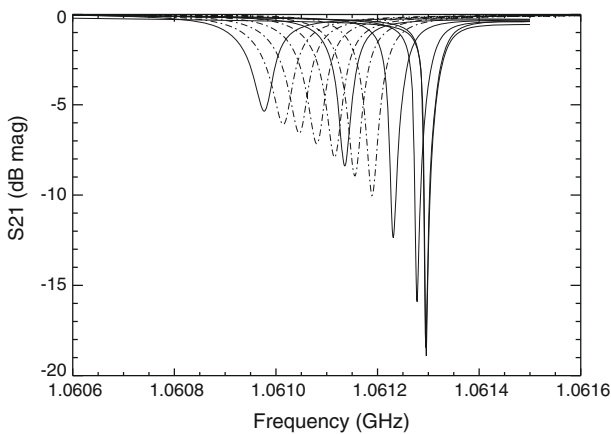


**Fig. 2** Magnitude of  $S_{21}$  as a function of frequency for different base temperature (*solid lines*) and optical loading (*dashed lines*). For the optically loaded measurements the base temperature was fixed at 245 mK. The input power at the device for all of the sweeps was approximately  $-78$  dBm

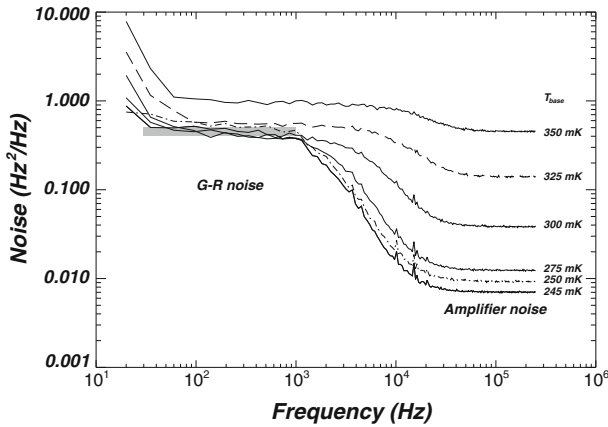


**Fig. 3** Measured noise for a dark NIKA pixel as a function of frequency for base temperatures from 245 to 350 mK. The low frequency part of the noise is dominated by generation–recombination (G–R) noise at the level expected from Mattis–Bardeen theory (grey box). The high frequency noise is dominated by amplifier noise. As the base temperature increases, the amplifier noise increases and the quasiparticle lifetime decreases causing the G–R noise to roll off at higher frequency

where  $I(\omega)$  and  $Q(\omega)$  are the Fourier transforms of the time stream  $I$  and  $Q$  data and  $dI/df$  and  $dQ/df$  are calculated from the frequency sweep data. The orthogonal linear combination of the raw  $I$  and  $Q$  data gives a signal that is proportional to the fluctuations in the quantity,  $1/q$ , and has a lower responsivity to changes in quasiparticle density and gives a flat noise spectrum with a level consistent with amplifier noise for frequencies above 10 Hz.

We fit the frequency noise data,  $e_f(\omega)$  over an audio frequency range of  $\omega/2\pi = 0.02–250$  kHz with a three component model consisting of a constant amplifier noise level plus a second noise term with a single pole rolloff corresponding to the quasiparticle lifetime. We find the amplifier noise levels for all noise measurements to be consistent with a 5 K noise temperature at the detector. From the cutoff frequencies, we calculate time constants ranging from approximately 10–100  $\mu$ s. For the dark noise data, we find a constant level for the second noise term of  $e_f^2 = 0.42 \pm 0.03$  Hz<sup>2</sup>/Hz. The expected G-R noise is given by  $e_f^2 = 4\beta^2 N_{qp} \tau_{qp}$  where  $\beta = df_0/dN_{qp}$  is the frequency responsivity,  $N_{qp}$  is the average number of quasiparticles in the material and  $\tau_{qp}$  is the quasiparticle lifetime. Because  $\tau_{qp} = \gamma/N_{qp}$ , where  $\gamma$  is a material constant, we expect the G–R noise to be constant over a temperature range where  $\beta$  is constant. Because we measure the frequency shift, the G–R frequency noise and the quasiparticle lifetime for different base temperatures, we can calculate a value for  $df_0/dN_{qp}$ . Given that for two different base temperatures,  $T_1$  and  $T_2$ ,  $N(T_1)\tau(T_1) = N(T_2)\tau(T_2)$  we find:

$$\frac{df_0}{dN_{qp}} = \frac{e_f^2 (1 - \tau(T_1)/\tau(T_2))}{4 (f(T_1) - f(T_2)) \tau(T_1)}. \tag{3}$$

From the dark data, we find a value of  $df_0/dN_{qp} = 0.036$  Hz/qp in good agreement with the estimate of the frequency responsivity assuming a quasiparticle density of

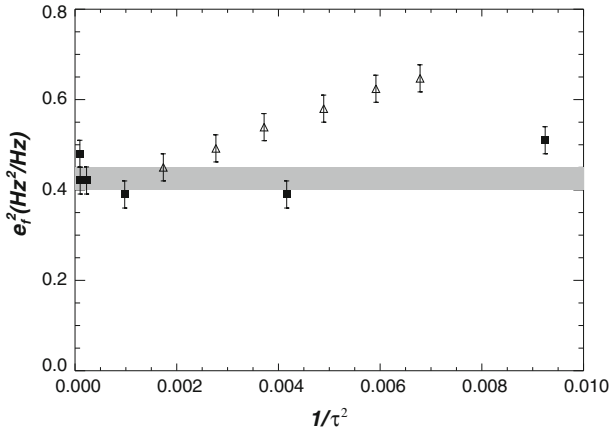


**Fig. 4** Amplitude of the measured low frequency white noise in a NIKA pixel as a function of the measured quantity,  $1/\tau_{qp}^2$ , where  $1/\tau_{qp}$  is proportional to the quasiparticle density which depends on both base temperature and incident optical power. The noise amplitude and quasiparticle lifetimes are determined from fits to the noise power spectra for the same pixel in the dark for different base temperature (*filled squares*) and for different levels of optical loading (*triangles*). The amplitude of the dark noise is roughly constant as a function of quasiparticle density as expected for G–R noise. The amplitude of the optical noise is equal to the dark noise at low optical loading as expected for incident photons which are capable of breaking a single Cooper pair and increases at higher loading indicating a contribution from photon correlations or wave noise

$$n_{qp} = 2N_0\sqrt{2\pi \Delta k_B T} \exp(-\Delta/k_B T) \tag{4}$$

where  $N_0$  is the single spin electron density of states at the Fermi energy, with  $N_0 = 1.72 \times 10^{10} \mu\text{m}^3 \text{eV}^{-1}$  and  $\Delta = 0.18 \text{ meV}$  for aluminum [1, 11, 12]. The optical data is very similar to the dark data and there is a low frequency component that rolls off to the amplifier noise level. The rolloff frequency increases as the temperature of the blackbody source increases. However, unlike the dark data, the low frequency white noise component also increases as the temperature of the blackbody source increases (Fig. 4) proportional to  $1/\tau_{qp}^2$ . For photon noise, we expect

$$e_f^2 \approx \gamma\beta^2 \left[ \left( \frac{h\nu}{\Delta} + 2 \right) + \frac{\gamma}{\tau_{qp}^2 \Delta \nu} \right] = A + \frac{B}{\tau_{qp}^2} \tag{5}$$

where the first term contains the photon shot noise and quasiparticle recombination noise and the second term is due to correlated photon wave noise. In the case where  $h\nu < 4\Delta$ , a single photon can only break one Cooper pair and the term  $h\nu/\Delta \rightarrow 2$  and the constant,  $A$  reduces to the same value as the G–R noise.

### 4 Conclusions

This is the first time that G–R noise and photon noise have been systematically measured with NIKA detectors. This measurement was made possible by improvement

in the sensitivity of NIKA detectors by using thinner aluminum films ( $\leq 20$  nm) and by developing a low noise laboratory test facility with a calibrated cryogenic blackbody source. Previous tests on NIKA arrays had all been carried out in the NIKA instrument cryostat that is designed to couple the detectors to the IRAM optics and uses a multiplexed detector readout with reduced signal bandwidth which does not allow measurement of the quasiparticle lifetimes. The measured noise of NIKA pixels appears to be limited by G–R noise in dark conditions and by photon noise when observing a blackbody source at frequencies above approximately 10–30 Hz. Below this frequency, the measurement is limited by noise sources which appear in both the frequency readout and the radius or quality factor readout which could be temperature fluctuations of the base plate or blackbody source or heating from mechanical vibrations from the pulse tube cryocooler. From the dark measurement of the G–R noise,  $e_f^{G-R}$ , the resonant frequency,  $f_0(T)$  and the quasiparticle lifetime,  $\tau(T)$  we can calculate the frequency response to change in quasiparticle number,  $df_0/dN_{qp}$ . We can use this to calculate the response of the KID to absorbed optical power,  $df_0/dP_{abs}$  and estimate the power absorbed by the KID. We can also estimate the absorbed power independently from the optical measurement of the photon noise in either the shot noise limit assuming that we know the effective wavelength of the absorbed radiation or in the wave noise limit assuming that we know the effective bandwidth of the absorbed radiation. These measurements demonstrate that it is possible to design and fabricate aluminum LEKIDs with close to photon-noise limited performance for instruments observing in the mm-wave bands.

**Acknowledgments** We acknowledge support from the UK STFC Grant Nos. ST/J001449/1 and ST/K000926/1, the French National Research Agency Grant No. ANR-09-JCJC-0021-01 and the EU SPACEKIDS project.

## References

1. P. Day, H. LeDuc, B. Mazin, A. Vayonakis, J. Zmuidzinis, *Nature* **425**, 817–820 (2003)
2. J.J.A. Baselmans, S.J.C. Yates, P. de Korte, H. Hoeffers, R. Barends, J.N. Hovenier, J.G. Gao, T.M. Klapwijk, *J. Adv. Space Res.* **40**, 708–713 (2007)
3. S. Doyle, P. Mauskopf, J. Naylon, A. Porch, C. Dunscombe, *JLTP* **151**, 530–536 (2008)
4. A. Monfardini, L. Swenson, A. Bidead, F.X. Desert, S.J.C. Yates, A. Benoit, A. Baryshev, J.J.A. Baselmans, S. Doyle, B. Klein, M. Roesch, C. Tucker, P.A.R. Ade, M. Calvo, P. Camus, C. Giordano, R. Guesten, C. Hoffman, S. Leclercq, P. Mauskopf, K.F. Schuster, *A&A* **521**, A29 (2010)
5. A. Monfardini, A. Benoit, A. Bidead, L. Swenson, A. Cruciani, P. Camus, C. Hoffman, F.X. Desert, S. Doyle, P. Mauskopf, C. Tucker, M. Roesch, S. Leclercq, K.F. Schuster, A. Endo, A. Baryshev, J.J.A. Baselmans, L. Ferrari, S.J.C. Yates, O. Bourrion, J. Macias-Perez, C. Vescovi, M. Calvo, C. Giordano, *ApJS* **194**, 24–35 (2011)
6. S. Golwala, C. Bocksteigel, S. Brugger, N.G. Czakon, P.K. Day, T.P. Downes, R. Duan, J. Gao, A. Gill, J. Glenn, M.I. Hollister, H.G. LeDuc, P.R. Maloney, B.A. Mazin, S.G. McHugh, D. Miller, O. Noroozian, H.T. Nguyen, J. Sayers, J.A. Schlaerth, S. Siegel, A.K. Vayonakis, P.R. Wilson, J. Zmuidzinis, in *Proceedings of SPIE*, vol. 8452 (SPIE, Bellingham, 2012), p. 845205
7. L.J. Swenson, P.K. Day, C.D. Dowell, B.H. Eom, M.I. Hollister, R. Jarnot, A. Kovacs, H.G. Leduc, C.M. McKenney, R. Monroe, T. Mroczkowski, H.T. Nguyen, J. Zmuidzinis, in *Proceedings of SPIE*, vol. 8452 (SPIE, Bellingham, 2012), p. 84520P-1
8. S. Heyminck, B. Klein, R. Guesten, C. Kasemann, A. Baryshev, J. Baselmans, S. Yates, T.M. Klapwijk, in *Twenty-First International Symposium on Space Terahertz Technology* (2010), p. 262.

9. S.J.C. Yates, J.J.A. Baselmans, A. Endo, R.M.J. Janssen, L. Ferrari, P. Diener, A.M. Baryshev, *Appl. Phys. Lett.* **99**, 073505 (2011)
10. M. Roesch, A. Benoit, A. Bidead, N. Boudou, M. Calvo, A. Cruciani, S. Doyle, H.G. Leduc, A. Monfardini, L. Swenson, S. Leclercq, P. Mauskopf, K.F. Schuster, in *Twenty-Second International Symposium on Space Terahertz Technology* (2011)
11. C.M. Wilson, L. Frunzio, D.E. Prober, *Phys. Rev. Lett.* **87**, 067004 (2001)
12. W. McMillan, *Phys. Rev.* **167**, 331 (1968)